Recombination and Reaction Dynamics Following Photodissociation of CH_3OCl in Solution

Christopher G. Elles, M. Jocelyn Cox, George L. Barnes, and F. Fleming Crim*

Department of Chemistry, University of Wisconsin − Madison, Madison, Wisconsin 53706

Received: July 28, 2004; In Final Form: September 21, 2004

We observe the dynamics of the products following the photodissociation of methyl hypochlorite (CH_3OCl) at 267 nm in solution. An ultraviolet charge-transfer transition reveals the evolution of Cl atoms in carbon tetrachloride, dichloromethane, 1,4-dichlorobutane, and chlorocyclohexane, and the data suggest that Cl atoms rapidly form a complex with the solvent. The Cl atom signal decays in 300 ps or less as a result of diffusive geminate recombination and bimolecular reaction. Diffusive geminate recombination consumes roughly 30% to 60% of the fragments that initially escape the solvent cage, while the remaining Cl atoms either react with excess CH_3OCl or abstract a hydrogen atom from the solvent. Reaction with CH_3OCl plays a significant role in carbon tetrachloride, dichloromethane, and 1,4-dichlorobutane, where the hydrogen abstraction reaction is relatively slow, but the faster decay of Cl atoms in chlorocyclohexane is a result of hydrogen abstraction from the solvent. A weak absorption due to the methoxy radical in cyclohexane, where we cannot probe the Cl atom directly, also shows evidence of diffusive geminate recombination and hydrogen abstraction from the solvent.

I. Introduction

The dynamics that occur following the photodissociation in solution often involve a complex series of reactions and relaxation processes.[1] In the photodissociation of ICN, for example, there is competition among geminate recombination, isomerization to form INC, and cage escape leading to the separated I and CN fragments.[2−4] Vibrational relaxation of the reforming ICN and INC molecules,[4] rotational relaxation of the nascent CN radical,[5] and hydrogen and chlorine abstraction from solvents such as chloroform[6] further complicate the dynamics. Complex dynamics are also evident following photodissociation of other small polyatomic molecules, such as I_3^-,[7,8] ClO_2,[9−11] HOCl,[12,13] and CH_2I_2,[14] although the specific details vary among these systems and depend on the solvent. Because many factors play a role in the outcome, exploring and comparing different cases potentially reveals the general principles that govern reactivity in solution. In this paper, we describe the dynamics that occur after 267-nm photodissociation of methyl hypochlorite (CH_3OCl) dissolved in several nonaqueous solvents.

Gas-phase studies of methyl hypochlorite provide a background for our measurements in solution. The ultraviolet absorption spectrum of gas-phase CH_3OCl has two weak bands, one centered at 235 nm and the other at 310 nm,[15] neither of which shift significantly upon solvation. Figure 1 shows the entire 310-nm absorption band and the low-energy edge of the 235-nm absorption band, which is about one order of magnitude stronger. A calculation of the electronic states by Li and Francisco[16] shows that all of the low-lying excited states (including the optically active $1^1A''$ and $2^1A'$ states) are directly dissociative along the O−Cl coordinate but bound along the C−O coordinate in the Franck−Condon region. Thus, electronic excitation in the gas phase dissociates the molecule, producing a ground electronic state methoxy radical and a chlorine atom.

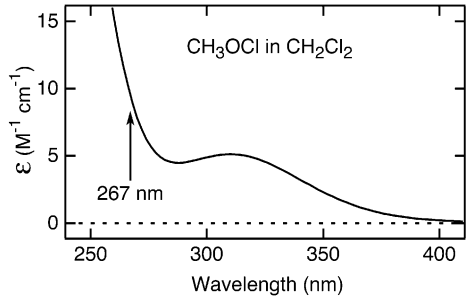

Figure 1. Electronic absorption spectrum of CH_3OCl in dichloromethane. The arrow indicates the photolysis wavelength of 267 nm.

$$CH_3OCl + h\nu \rightarrow CH_3O\ (\tilde{X}^2E) + Cl\ (^2P) \qquad (1)$$

The quantum yield for this reaction is near unity (0.95 ± 0.05),[17] and Krisch et al.[18] report that photodissociation of jet-cooled CH_3OCl at 248 nm deposits 48 kcal/mol of energy in relative translation of the fragments and 20 kcal/mol in rotation of the methoxy radical.

Translational energy is important for photodissociation reactions in solution, where the solvent acts as a barrier to the separation of the fragments. Keiding and co-workers[12] examine the dynamics following the dissociation of HOCl in water and find that the kinetic energy of the fragments is sufficient for escape from the solvent cage. They monitor the evolution of the Cl atom via the Cl−water charge-transfer transition[19] centered at 315 nm and observe diffusive geminate recombination on a time scale of roughly 50 ps for nearly one-half of the Cl atoms that initially escape the solvent cage. Within 200 ps, about 10% of the remaining Cl atoms react with HOCl to form Cl_2 and OH, but a strong residual absorption in the transient

* Corresponding author. E-mail: fcrim@chem.wisc.edu.

10.1021/jp046627b CCC: $27.50
Published on Web 11/18/2004

spectrum implies that many Cl atoms remain unreacted on the time scale of the measurement. In a second study, Keiding and co-workers[13] show that the fraction of unreacted Cl atoms increases with increasing photolysis energy, because additional translational energy in the fragments causes them to separate to a greater distance before equilibrating with the solvent. The gas-phase dissociation of CH_3OCl is very similar to that of HOCl,[17] but unlike HOCl, which is difficult to dissolve in solvents other than water, CH_3OCl is readily synthesized in any solvent that is immiscible with water. Our inability to incorporate the two species in the same solvent complicates the direct comparison of the dynamics following dissociation, but the ability to change the solvent in the case of CH_3OCl allows us to examine its influence on the dissociation and recombination dynamics directly.

Our experiments monitor the evolution of the system after the photodissociation of CH_3OCl in carbon tetrachloride (CCl_4), dichloromethane (CH_2Cl_2), 1,4-dichlorobutane ($C_4H_8Cl_2$), chlorocyclohexane ($C_6H_{11}Cl$), and cyclohexane (C_6H_{12}). In the chlorinated solvents, we measure the absorption due to a charge-transfer transition between the nascent Cl atom and the solvent.[20] The photodissociation of CH_3OCl is prompt, and although we do not have sufficient time resolution to observe the initial increase of the signal directly, the transient absorption continues to rise over the first few picoseconds of the measurement in some solvents. As we will describe in the following text, we attribute the increase in absorption to the formation and relaxation of a ground-state Cl−solvent complex. The subsequent decay of Cl atoms is a result of diffusive geminate recombination and diffusion-limited reaction with excess hypochlorite, except in the case of chlorocyclohexane, where a significantly faster decay suggests that hydrogen abstraction from the solvent also plays a role. We are unable to probe the Cl atom directly in cyclohexane and instead observe a weak absorption due to the methoxy radical, which provides evidence for both geminate recombination of the fragments and hydrogen abstraction from the solvent by Cl atoms.

II. Experimental Approach

We dissociate CH_3OCl with a 267-nm laser pulse and measure the transient change in absorption with a tunable UV probe pulse. The 100-fs pump and probe pulses come from the nonlinear frequency conversion of the 800-nm fundamental of a regeneratively amplified Ti:sapphire laser (Clark MXR CPA-1000), which produces 0.8-mJ pulses at a repetition rate of 1 kHz. Successive Type I β-barium borate (BBO) crystals (300 μm, $\theta = 29°$; and 200 μm, $\theta = 42°$) convert about half of the Ti:sapphire fundamental into 267-nm light by frequency doubling and mixing, respectively. An optical parametric amplifier and two successive Type I BBO doubling crystals (1 mm, $\theta = 22°$; and 300 μm, $\theta = 29°$) generate probe pulses that are tunable down to 290 nm. We adjust the relative delay between the pump and probe pulses with a computer-controlled translation stage, and an optical chopper blocks every other pump pulse for active background subtraction. The sample circulates through a flow cell with a 1-mm path length and 2-mm-thick quartz windows. A 300-mm lens focuses the probe beam to a diameter of 140 μm in the cell, where it intersects the 800-μm-diameter pump beam at a small angle. We attenuate the pump pulse to ensure that the transient signal from two-pump photon absorption in the solvent is less than 0.1 mOD and average between 1000 and 2000 laser shots per point to give a noise level of about 0.05 mOD. The cross-correlation of the pump and probe pulses has a width of about 500 fs (fwhm) due to group velocity dispersion in the sample and the noncollinear geometry of the experiment.

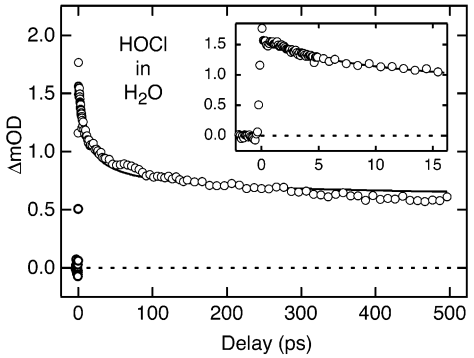

Figure 2. Transient absorption at 310 nm following photodissociation of HOCl in water. The solid line is a fit to the data using eq 2.

We synthesize methyl hypochlorite using the procedure of Jenner[21] with minor modifications. We add 16 mL of methanol and 24 mL of glacial acetic acid to about 150 mL of solvent at 0 °C. After mixing the solution for 5 min, we add 300 mL of aqueous NaOCl (Ultra Clorox Bleach) and stir vigorously for another 5 min. Discarding the aqueous layer and washing the organic layer with a solution of sodium bicarbonate neutralizes any remaining acetic acid and yields the solution of methyl hypochlorite. Typically, we dilute the solution to a concentration of 1.1 M, corresponding to an optical density of 1.0 for the 267-nm pump pulse in the 1-mm path-length cell. We use all reagents and solvents from commercial sources without further purification.

III. Results and Analysis

A. HOCl. We first examine the dynamics following 267-nm photodissociation of HOCl in water to provide a point of comparison. The transient absorption that we observe at a probe wavelength of 315 nm (the peak absorption of the Cl−solvent charge-transfer transition in water)[19] closely resembles that of Keiding and co-workers,[12,13] who extensively investigated the dynamics following the photodissociation of aqueous HOCl. The signal, shown in Figure 2, decays nonexponentially in about 50 ps to roughly one-half of the initial intensity, and we fit the data using a model similar to that of Keiding and co-workers.[12] The model for diffusion-limited recombination of an isolated pair of radicals assumes that the photodissociation fragments equilibrate with the solvent at a distance of r_0 and that they recombine with unit probability at a reaction radius of R_{recomb}.[22,23] The time-dependent Cl atom signal is

$$A_{Cl}(t) = A_{Cl}(0)\cdot\left[1 - \frac{R_{recomb}}{r_0}\,\mathrm{erfc}\left(\frac{r_0 - R_{recomb}}{\sqrt{4D_{recomb}t}}\right)\right] \qquad (2)$$

where D_{recomb} is the relative diffusion coefficient of the fragments ($D_{recomb} = D_{Cl} + D_{MeO}$). The fit to the data in Figure 2 using the diffusion constant ($D_{recomb} = 3.0$ nm^2/ns) and reaction radius ($R_{recomb} = 0.35$ nm) of Keiding and co-workers[13] yields an initial separation of $r_0 = 0.56$ nm, in excellent agreement with the equilibration distance that they report. Because the complementary error function approaches unity in the long time limit, the value $(1 - R_{recomb}/r_0) = 0.37$ indicates that approximately 37% of the Cl atoms survive and 63% geminately recombine with the hydroxy radical. The fit slightly overestimates the recombination yield and does not precisely

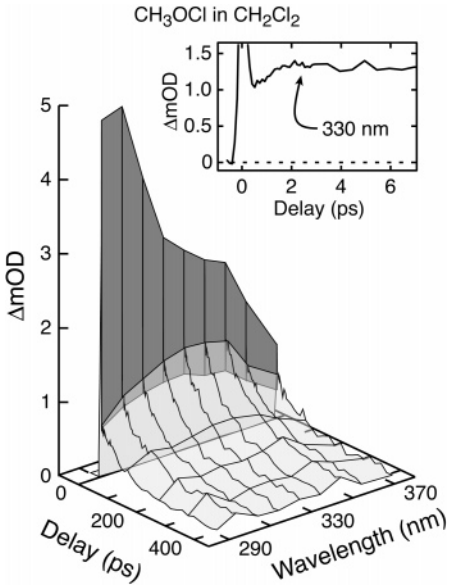

Figure 3. Transient absorption spectrum of the Cl−solvent complex as a function of the delay following photodissociation of CH_3OCl in dichloromethane. The inset shows the first 7 ps of the transient absorption at 330 nm.

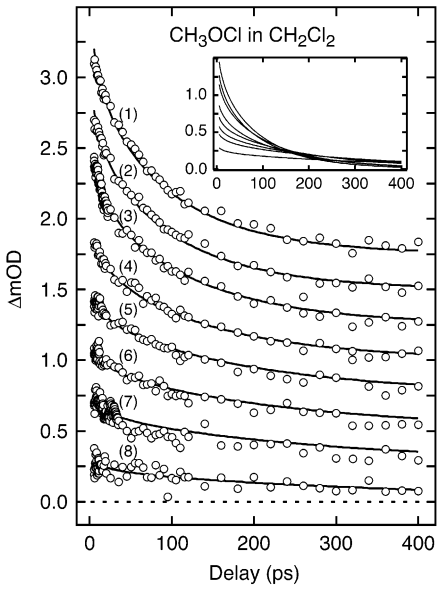

Figure 4. Transient absorption at 330 nm following photodissociation of various concentrations of CH_3OCl in dichloromethane. The solid lines are a simultaneous fit of all eight traces using eq 7 and the values in Table 1. The traces are offset from each other by 0.25 mOD for clarity, except in the inset, which shows the fit without the data.

reproduce the tail for longer delays, because we ignore the small fraction of Cl atoms that react with HOCl to form Cl_2 and OH.

B. CH_3OCl. The data in Figure 3 show the evolution of the transient absorption spectrum following photolysis of CH_3OCl in dichloromethane. There is a wavelength-dependent two-photon solvent absorption when the pump and probe pulses overlap in time, but for positive delays, we observe a transient absorption, centered at about 330 nm, corresponding to a Cl−solvent charge-transfer transition.[20] The inset in Figure 3 shows the transient absorption at 330 nm for the first several picoseconds after dissociation. Two-photon solvent absorption obscures the initial increase of the signal, but there is also a second, slower rise over the next 2 ps, after which the Cl atom signal decays to the baseline. The complete decay of the signal within about 300 ps contrasts with the observation of relatively long-lived Cl atoms following the photodissociation of aqueous HOCl.

The rise of the signal likely reflects the formation and relaxation of a complex between the Cl atom and a solvent molecule, as discussed in the following text. The decay of the signal, on the other hand, indicates the disappearance of Cl atoms through a combination of diffusive geminate recombination and reaction. Diffusive geminate recombination alone cannot explain the return of the signal to the baseline, because at least some of the fragment pairs should diffuse apart from each other, as is the case for HOCl. Therefore, either the initial separation of methoxy and Cl radicals is insufficient for diffusion to control the recombination, or the Cl atoms disappear through a different mechanism. In fact, Cl atoms can undergo several reactions, including hydrogen and chlorine abstraction from the solvent,

$$Cl + CH_2Cl_2 \rightarrow HCl + CHCl_2 \quad (3)$$

$$Cl + CH_2Cl_2 \rightarrow Cl_2 + CH_2Cl \quad (4)$$

or reaction with excess methyl hypochlorite

$$Cl + CH_3OCl \rightarrow Cl_2 + CH_3O \quad (5)$$

We exclude reactions with dichloromethane on the time scale of our measurements, since Alfassi et al.[24] reported a 5-ns half-life for Cl atoms in that solvent. Reaction with methyl hypochlorite, on the other hand, is a likely means of removing Cl atoms, because it proceeds rapidly in the gas phase,[25] and the high concentration of CH_3OCl in our experiment makes a diffusive encounter with the Cl atom likely.

The Smoluchowski theory for diffusion-limited bulk reactions describes the decay of Cl atoms due to reaction with excess hypochlorite[22,23]

$$A_{Cl}(t) = A_{Cl}(0)\cdot\exp\left[-4\pi R_{rxn} D_{rxn} c_{ROCl}\left(t + 2R_{rxn}\sqrt{\frac{t}{\pi D_{rxn}}}\right)\right] \quad (6)$$

an expression that depends on the concentration of undissociated CH_3OCl, c_{ROCl}. In an analogy with pure diffusive recombination (eq 2), D_{rxn} is the relative diffusion coefficient (for Cl and CH_3OCl), and R_{rxn} is the radius within which the species react with unit probability. To test the concentration dependence, we examine the decay for initial CH_3OCl concentrations ranging from 0.4 to 1.5 M, as shown in Figure 4. Fitting the data with eq 6 does not adequately describe the decay of Cl atoms, however, because it omits the contribution from diffusive geminate recombination. We instead write the full expression for the decay of Cl atoms following the photodissociation of CH_3OCl in solution, using the pair survival probability formulation[23] to account for both geminate recombination and reaction.

$$A_{Cl}^{(n)}(t) = A_{Cl}^{(n)}(0)\cdot\left[1 - \frac{R_{recomb}}{r_0}\,\mathrm{erfc}\left(\frac{r_0 - R_{recomb}}{\sqrt{4D_{recomb}t}}\right)\right]\cdot \exp\left[-4\pi R_{rxn} D_{rxn} c_{ROCl}^{(n)}\left(t + 2R_{rxn}\sqrt{\frac{t}{\pi D_{rxn}}}\right)\right] \quad (7)$$

Extrapolating the data to zero delay gives the initial amplitudes, $A_{Cl}^{(n)}(0)$, and we simultaneously fit all eight traces in Figure 4 (solid lines), allowing only the recombination radius, R_{recomb}, and the reaction radius, R_{rxn}, to vary. (The superscript n refers to the particular trace, $1 \le n \le 8$.) We use the Stokes−Einstein

TABLE 1: Fitting Parameters for the Data in Figure 4

	Adjustable Parameters[a]		
R_{recomb}	0.20 nm	R_{rxn}	0.10 nm
	Constant Parameters		
r_0	0.6 nm		
D_{recomb}	5.2 nm^2/ns	D_{rxn}	4.7 nm^2/ns
$A_{Cl}^{(1)}(0)$	1.58 mOD	$c_{ROCl}^{(1)}$	1.5 M
$A_{Cl}^{(2)}(0)$	1.36 mOD	$c_{ROCl}^{(2)}$	1.4 M
$A_{Cl}^{(3)}(0)$	1.23 mOD	$c_{ROCl}^{(3)}$	1.2 M
$A_{Cl}^{(4)}(0)$	0.92 mOD	$c_{ROCl}^{(4)}$	1.0 M
$A_{Cl}^{(5)}(0)$	0.73 mOD	$c_{ROCl}^{(5)}$	0.7 M
$A_{Cl}^{(6)}(0)$	0.59 mOD	$c_{ROCl}^{(6)}$	0.6 M
$A_{Cl}^{(7)}(0)$	0.48 mOD	$c_{ROCl}^{(7)}$	0.5 M
$A_{Cl}^{(8)}(0)$	0.30 mOD	$c_{ROCl}^{(8)}$	0.4 M

[a] Approximate uncertainty in R_{recomb} and R_{rxn} is 0.05 nm.

equation[22] to calculate the diffusion constants of $D_{recomb} = 5.2$ nm^2/ns and $D_{rxn} = 4.7$ nm^2/ns for the recombination and bulk reaction, respectively, and a rudimentary molecular dynamics simulation suggests an initial fragment separation of $r_0 = 0.6$ nm.[26,27] Table 1 lists all of the values for the linear least-squares fit of the data in Figure 4.

The values for R_{rxn} and R_{recomb} that we obtain from fitting the data in Figure 4 are too small. They are shorter than the eventual Cl_2 bond length and roughly the same as the O−Cl bond length of the recombined molecule, respectively. More reasonable values for the reaction and recombination radii are the distances at which the attractive potentials of the fragments are k_BT below the asymptotic limit, because thermal energy is insufficient to overcome the attraction between the fragments within this distance. One explanation for the short radii is that the diffusion constants that we calculate are too large, and the fit compensates with short reaction radii. The Stokes−Einstein equation is only an approximatation and probably overestimates the value of the diffusion constant, because the Cl atom forms a complex with the solvent. Alternatively, the short radii may indicate that the recombination and reaction do not occur on every encounter. Collins and Kimball[28] treat the latter possibility, the reflective boundary condition, and show that R_{rxn} (and R_{recomb}, by analogy) is an effective radius that accounts for the finite probability of reaction on every encounter.[22] In the present experiment, this situation could result from the nonspherical symmetry of the reactants,[29,30] because the Cl atom must encounter the oxygen on the methoxy radical or the chlorine on the hypochlorite molecule for the recombination or reaction to occur. The geometry of the approach does not play as large of a role in the case of HOCl because of the smaller size of hydrogen compared to a methyl group.

We also study the dissociation of CH_3OCl in carbon tetrachloride (CCl_4), 1,4-dichlorobutane ($C_4H_8Cl_2$), and chlorocyclohexane ($C_6H_{11}Cl$) to examine the influence of the solvent on the recombination and reaction dynamics of Cl atoms. Figure 5 compares the transient absorption at 330 nm for each of these solvents and dichloromethane, including insets of the initial 20 ps. We observe the secondary, few-picosecond rise in dichloromethane and dichlorobutane, but not in carbon tetrachloride or chlorocyclohexane, where the rise of the signal occurs entirely within the solvent response (less than 1 ps). On a longer time scale, the nonexponential decay of the signal is similar for solutions of CH_3OCl in carbon tetrachloride, dichloromethane, and dichlorobutane, returning to the baseline in about 300 ps. The signal decays more rapidly in chlorocyclohexane, where the Cl atoms disappear in substantially less than 100 ps. (The small offset beyond 100 ps is a result of two-pump photon absorption by the solvent and occurs even in the absence of CH_3OCl.) The solid lines in the top three traces of Figure 5 are fits to the data using eq 7 and the values in Table 2, where R_{recomb} and R_{rxn} are the only adjustable parameters. We know the concentration of CH_3OCl for each trace, the Stokes−Einstein equation gives the diffusion constants, and we use $r_0 = 0.6$ nm, the value from our molecular dynamics simulation. Tables 1 and 2 list values of R_{recomb} and R_{rxn} for CH_3OCl in dichloromethane that differ by 0.02 and 0.05 nm, respectively, because they come from fitting different sets of data. This difference indicates the degree of uncertainty in our results.

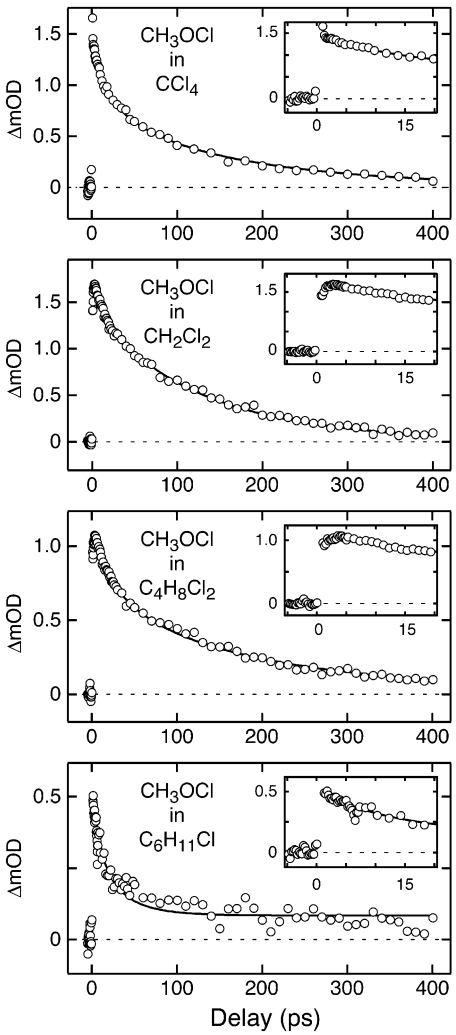

Figure 5. Transient absorption at 330 nm following photodissociation of CH_3OCl in carbon tetrachloride, dichloromethane, 1,4-dichlorobutane, and chlorocyclohexane. The solid lines are fits to the data using eq 7 and the parameters in Table 2.

TABLE 2: Fitting Parameters for Figures 5 and 6

	adjustable parameters[a]		constant parameters				
solvent	R_{recomb} nm	R_{rxn} nm	r_0 nm	D_{recomb} nm^2/ns	D_{rxn} nm^2/ns	$A_{Cl}(0)$ mOD	c_{ROCl} M
CCl_4	0.35	0.25	0.6	2.4	2.1	1.47	1.1
CH_2Cl_2	0.22	0.15	0.6	5.2	4.7	1.80	1.1
$C_4H_8Cl_2$	0.33	0.29	0.6	1.7	1.5	1.17	1.0
$C_6H_{11}Cl$[b]	0.33[b]	0.23	0.6	1.7	1.5	0.49	8.4[b]
C_6H_{12}[c]	0.37		0.6	2.2		0.51	

[a] Approximate uncertainty in R_{recomb} and R_{rxn} is 0.05 nm. [b] The fit for $C_6H_{11}Cl$ assumes that Cl atoms react with the solvent, rather than CH_3OCl, and includes an offset of 0.08 mOD to account for the background signal. R_{recomb} is held constant, and the concentration of the solvent replaces c_{ROCl}. [c] Fit with the pure recombination model (eq 2).

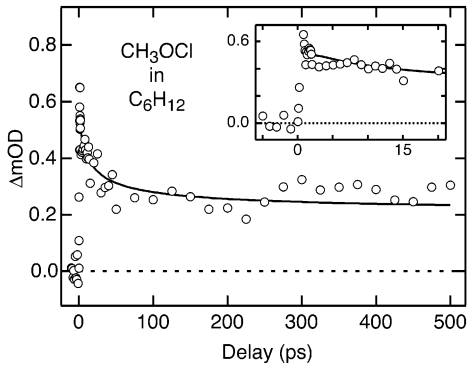

Figure 6. Transient absorption at 267 nm following photodissociation of CH_3OCl in cyclohexane. The solid line is a fit to the data using eq 2 and the parameters in Table 2.

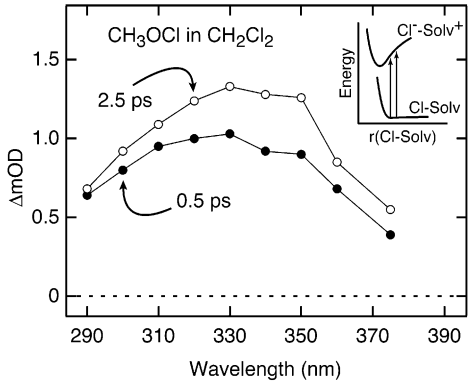

Figure 7. Transient absorption spectrum of the Cl−solvent complex at 0.5 and 2.5 ps after photodissociation of CH_3OCl in dichloromethane.

The fast decay of the Cl atom signal in chlorocyclohexane (bottom of Figure 5) suggests that hydrogen abstraction from the solvent, in addition to recombination and reaction with excess methyl hypochlorite, consumes Cl atoms. To fit the data, we modify eq 7 to include the hydrogen abstraction reaction

$$Cl + C_6H_{11}Cl \rightarrow HCl + C_6H_{10}Cl \qquad (8)$$

rather than the slower reaction with excess methyl hypochlorite. The primary difference is that R_{rxn} and D_{rxn} are the reaction radius and relative diffusion constant for a Cl atom and a chlorocyclohexane molecule, and we substitute the concentration of the solvent for c_{ROCl}. We also include an offset of 0.08 mOD in the fit to account for the solvent background. After setting R_{recomb} equal to 0.33 nm (the result from the most similar solvent, dichlorobutane) and using the parameters in Table 2, we obtain a best fit to the data with a value of $R_{rxn} = 0.23$ nm. Not surprisingly, the effective reaction radius, R_{rxn}, is unphysically short, because an activation barrier limits the hydrogen abstraction reaction.[22,28]

In the non-chlorinated solvent, cyclohexane, we are not able to observe the Cl−solvent charge-transfer transition and, thus, cannot monitor the dynamics of the Cl atom. Although the ionization potential of cyclohexane and the transition energies for other halogen atom−solvent charge-transfer transitions suggest an absorption near 450 nm,[20,31] the transition may be too weak to detect in our experiment. Instead, we observe the evolution of the methoxy radical using its weak absorption below about 315 nm.[32] (Detecting Cl_2 is impossible in all of the solvents because of its low absorptivity.[33,34]) Figure 6 shows the transient absorption at a probe wavelength of 267 nm following the photodissociation of CH_3OCl (also at 267 nm) in cyclohexane. After an initial decay over the first 50 ps, the methoxy signal remains roughly constant for delay times as long as 500 ps. The line through the data is a best fit using the pure recombination model of eq 2 with $D_{recomb} = 2.2$ nm^2/ns and $r_0 = 0.6$ nm to give $R_{recomb} = 0.37$ nm.

IV. Discussion

A. Formation of a Cl−Solvent Complex. The transient absorption that we observe following the photodissociation of CH_3OCl in chlorinated solvents reveals the presence of Cl atoms via a Cl−solvent charge-transfer transition. This signal reaches a maximum within the solvent response time for two of the solvents, carbon tetrachloride and chlorocyclohexane, but we also observe a slower, few-picosecond rise of the signal in dichloromethane and dichlorobutane. Earlier reports[35,36] show that Cl atoms form a weak complex with various chlorinated solvents, and we attribute both the initial, unresolved rise of the signal and the secondary increase to the formation and relaxation of this complex. The absorption increases as the complex forms and relaxes because the charge-transfer transition becomes more favorable with decreasing Cl−solvent separation.

Figure 7 shows the spectrum of the charge-transfer transition at 0.5 and 2.5 ps after the photodissociation of CH_3OCl in dichloromethane. The intensity increases more on the low-energy side of the spectrum than on the high-energy side, indicating a slight shift as the complex relaxes. This result resembles the usual observation that the electronic spectrum narrows upon vibrational relaxation, but in this case, the spectrum shifts to lower energy because of the shape of the excited-state potential energy surface. The ionic excited state has a minimum at shorter Cl−solvent separation than the ground state, and because the energy level of the excited state changes more dramatically with bond length than the weakly bound ground state, the energy difference between states decreases with decreasing separation.

The slightly different time scales for the slow rise of the Cl atom signal in dichloromethane and dichlorobutane, as well as the apparent absence of a secondary increase in carbon tetrachloride and chlorocyclohexane, reflect a difference in the formation of the Cl−solvent complex. Many factors depend on the solvent, including the rate of energy dissipation and the strength of the complex. As a result, the time scale for complex formation and relaxation is different in each solvent. The Cl signal from the photolysis of aqueous HOCl appears within the solvent response, as shown in Figure 2. In the case of HOCl, however, Keiding and co-workers[12] report a signal rise time of about 1 ps for probe wavelengths longer than 340 nm, where the two-photon solvent absorption is negligible and does not interfere with the measurement. This time scale is slower than the dissociation of HOCl to form a Cl atom (less than a few hundred femtoseconds) and, instead, reflects the formation and relaxation of a Cl−water complex, just as we observe for CH_3OCl in the chlorinated solvents.

B. Geminate Recombination and Bimolecular Reaction. Both diffusive geminate recombination and bimolecular reaction contribute to the decay of Cl atoms that we observe following the photodissociation of CH_3OCl in chlorinated solvents. Geminate recombination plays an important role in most solution-phase photodissociation reactions, because the solvent impedes the separation of the fragments. Solvent "caging", for instance, can trap the nascent pair within the original solvation shell and lead to recombination on a time scale of a few picoseconds or less.[1] In the present case, however, the fragments that we observe have enough kinetic energy to escape the solvent cage, and the limiting step in the recombination is the relative

diffusion of the fragments. An important consequence of cage escape is that some of the fragments diffuse away from each other, often reacting with other solute molecules or with the solvent.

The dynamics following the photolysis of aqueous HOCl are a good example of diffusive geminate recombination, because a significant fraction of the fragments do not recombine, and no other reaction plays a significant role on the time scale of the recombination. The roughly 50-ps decay of the Cl atom signal in Figure 2 indicates that about one-half of the fragments geminately recombine, while the relatively constant signal at longer delays shows the long lifetime for Cl atoms that escape recombination. Fitting the data with eq 2 allows us to quantify the branching between survival and recombination, because the ratio R_{recomb}/r_0 is equal to the fraction of particles that recombine. The best fit to the data yields $R_{recomb}/r_0 = 0.63$, or 63% recombination, assuming a recombination radius of $R_{recomb} = 0.35$ nm.[13] Our fit to the data oversimplifies the dynamics, because we do not account for a distribution of values for r_0, and we ignore the reaction of Cl atoms with excess HOCl, but the result agrees well with that of Keiding and co-workers,[13] who treat both of these issues.

The situation is not as clear following the photodissociation of CH_3OCl, where geminate recombination alone cannot describe the decay of the Cl atom signal to the baseline, and we must also consider other reactions. Because of the high concentration of undissociated methyl hypochlorite, we expect that chlorine abstraction from CH_3OCl to form Cl_2 (reaction 5) plays an important role in the decay of Cl atoms, particularly when reaction with the solvent is much slower. It is difficult to distinguish the contributions from geminate recombination and the bimolecular reaction, because they occur on similar time scales, but changing the concentration of CH_3OCl reveals the competition between these decay channels. The inset in Figure 4 shows the fits without the data and demonstrates that the signal approaches the baseline more rapidly for higher concentrations of methyl hypochlorite, where the bimolecular reaction is faster. The contribution from geminate recombination does not change with concentration, and we obtain $R_{recomb}/r_0 = 0.33$ from the fit to the data in Figure 4, indicating that about 33% of the fragments geminately recombine and the remaining 67% react with undissociated CH_3OCl. Interestingly, the fit gives a steady-state bimolecular reaction rate constant[22]

$$k(t)|_{t\to\infty} = 4\pi R_{rxn} D_{rxn}\left(1 + \frac{R_{rxn}}{\sqrt{\pi D_{rxn} t}}\right)|_{t\to\infty} = 4\pi R_{rxn} D_{rxn} \qquad (9)$$

of 4×10^9 M^{-1} s^{-1}, which is an order of magnitude slower than the gas-phase rate constant of 3.7×10^{10} M^{-1} s^{-1} for the reaction of Cl atoms with CH_3OCl.[25] This difference indicates that the solvent inhibits the reaction, similar to the observation by Raftery et al.[37] that the rate of hydrogen abstraction from cyclohexane in solution is 14 times slower than in the gas phase. The slower reaction in solution may be the result of a larger barrier to reaction in the presence of solvent, possibly due to the formation of a Cl−solvent complex. Fitting the data in Figure 5 gives similar rate constants for the reaction of Cl atoms with CH_3OCl in carbon tetrachloride and dichlorobutane, and Table 3 lists these results as well as the recombination yields for each solvent.

Previous measurements of the Cl atom lifetime in dichloromethane[24] (∼5 ns) and carbon tetrachloride[38] (172 ns) support our interpretation that the reaction with undissociated methyl hypochlorite is the primary decay mechanism for Cl atoms that do not geminately recombine in these solvents. The faster decay of the Cl atom signal in chlorocyclohexane, on the other hand, is a result of hydrogen abstraction from the solvent. Raftery et al.[37] report a 20-ps time scale for hydrogen abstraction from cyclohexane

$$Cl + C_6H_{12} \rightarrow HCl + C_6H_{11} \qquad (10)$$

and it is not unreasonable to expect a similar reaction rate for chlorocyclohexane (reaction 8). In fact, fitting the bottom trace in Figure 5 gives a steady-state reaction rate constant of 2×10^9 M^{-1} s^{-1} for hydrogen abstraction from chlorocyclohexane, corresponding to a lifetime of about 50 ps.

Although we cannot measure the hydrogen abstraction rate in cyclohexane directly, the methoxy radical signal in Figure 6 provides evidence that hydrogen abstraction by the Cl atom (reaction 10) also plays a role in this solvent. The partial decay of the methoxy signal over the initial 50 ps is consistent with the geminate recombination of slightly more than half of the photodissociation fragments, but the constant signal beyond ∼50 ps suggests that Cl atoms do not react with excess CH_3OCl, because that reaction would lead to a net increase in methoxy radicals. Hydrogen abstraction from the solvent provides an alternate decay channel for Cl atoms that does not affect the concentration of methoxy radicals. The 20-ps time scale that Raftery et al.[37] find for hydrogen abstraction from cyclohexane is consistent with this observation, because that reaction removes Cl atoms from solution before they react with excess methyl hypochlorite.

TABLE 3: Recombination Yield and Steady-State Bimolecular Reaction Rate Constants[a]

solvent	R_{recomb}/r_0	$4\pi R_{rxn} D_{rxn}$ M^{-1} s^{-1}	reaction
CCl_4	0.58	4.0×10^9	$CH_3OCl + Cl$
CH_2Cl_2	0.37	5.2×10^9	$CH_3OCl + Cl$
CH_2Cl_2[b]	0.33	3.6×10^9	$CH_3OCl + Cl$
$C_4H_8Cl_2$	0.55	3.3×10^9	$CH_3OCl + Cl$
$C_6H_{11}Cl$	0.55[c]	2.3×10^9	$C_6H_{11}Cl + Cl$
C_6H_{12}[d]	0.62		

[a] Uncertainty is approximately 0.08 in R_{recomb}/r_0 and 0.5×10^9 M^{-1} s^{-1} in the rate constant. [b] From the fit to the data in Figure 4. [c] Fixed value. [d] From the fit to the data in Figure 6 using the pure recombination model (eq 2).

V. Summary

The dynamics following the photodissociation of CH_3OCl in solution include the formation of a Cl−solvent complex, diffusive geminate recombination, and bimolecular reaction. The weak complex between the nascent Cl atom and the solvent forms and relaxes in a few picoseconds or less, resulting in an increase in the intensity of a Cl−solvent charge-transfer transition. In some chlorinated solvents, the rise occurs entirely within the solvent response time, while in others, we observe a secondary increase in the signal height that takes a few picoseconds. The Cl atom signal then decays to the baseline in 300 ps or less, depending on the solvent. Roughly 30−60% of the fragments that initially escape the solvent cage diffusively reencounter each other and geminately recombine. All of the remaining Cl atoms either react with excess CH_3OCl or abstract a hydrogen atom from the solvent.

The diffusive geminate recombination of Cl atom and methoxy radical pairs is similar to the recombination that occurs following the photodissociation of aqueous HOCl. The Cl atoms that survive recombination have a longer lifetime in the latter

case, however, because they react with undissociated HOCl in water much more slowly than with undissociated CH_3OCl in nonaqueous solvents. Additionally, hydrogen abstraction further accelerates the decay of Cl atoms in some of the nonaqueous solvents. Reaction with CH_3OCl occurs with a rate constant of about $(3-5) \times 10^9$ M^{-1} s^{-1} in carbon tetrachloride, dichloromethane, and 1,4-dichlorobutane, where the hydrogen abstraction reaction is relatively slow. In chlorocyclohexane, on the other hand, hydrogen abstraction from the solvent consumes the remaining Cl atoms with a steady-state rate constant of 2×10^9 M^{-1} s^{-1}. Although this rate constant is slightly smaller than the rate constant for the reaction of Cl atoms with CH_3OCl, the hydrogen abstraction reaction dominates because of the higher concentration of chlorocyclohexane. The dynamics of the methoxy radical in cyclohexane are also consistent with diffusive geminate recombination and hydrogen abstraction from the solvent. In the case of cyclohexane, we cannot directly observe the disappearance of Cl atoms, but hydrogen abstraction is known to occur with a rate constant of 5.6×10^9 M^{-1} s^{-1}. Our measurements on CH_3OCl demonstrate that complex dynamics occur after photodissociation, including competition among several processes, and highlight the importance of the solvent in determining the outcome.

Acknowledgment. We are grateful to Leonid Sheps and Andrew Crowther for many helpful discussions. This work is supported by the Air Force Office of Scientific Research.

References and Notes

(1) Harris, A. L.; Brown, J. K.; Harris, C. B. *Annu. Rev. Phys. Chem.* **1988**, *39*, 341.
(2) Benjamin, I. *J. Chem. Phys.* **1995**, *103*, 2459.
(3) Wan, C. Z.; Gupta, M.; Zewail, A. H. *Chem. Phys. Lett.* **1996**, *256*, 279.
(4) Larsen, J.; Madsen, D.; Poulsen, J. A.; Poulsen, T. D.; Keiding, S. R.; Thogersen, J. *J. Chem. Phys.* **2002**, *116*, 7997.
(5) Moskun, A. C.; Bradforth, S. E. *J. Chem. Phys.* **2003**, *119*, 4500.
(6) Raftery, D.; Gooding, E.; Romanovsky, A.; Hochstrasser, R. M. *J. Chem. Phys.* **1994**, *101*, 8572.
(7) Banin, U.; Ruhman, S. *J. Chem. Phys.* **1993**, *98*, 4391.
(8) Kuhne, T.; Vohringer, P. *J. Chem. Phys.* **1996**, *105*, 10788.
(9) Thogersen, J.; Thomsen, C. L.; Poulsen, J. A.; Keiding, S. R. *J. Phys. Chem. A* **1998**, *102*, 4186.
(10) Thomsen, C. L.; Philpott, M. P.; Hayes, S. C.; Reid, P. J. *J. Chem. Phys.* **2000**, *112*, 505.
(11) Philpott, M. P.; Hayes, S. C.; Thomsen, C. L.; Reid, P. J. *Chem. Phys.* **2001**, *263*, 389.
(12) Thomsen, C. L.; Madsen, D.; Poulsen, J. A.; Thogersen, J.; Jensen, S. J. K.; Keiding, S. R. *J. Chem. Phys.* **2001**, *115*, 9361.
(13) Madsen, D.; Thomsen, C. L.; Poulsen, J. A.; Jensen, S. J. K.; Thogersen, J.; Keiding, S. R.; Krissinel, E. B. *J. Phys. Chem. A* **2003**, *107*, 3606.
(14) Tarnovsky, A. N.; Alvarez, J. L.; Yartsev, A. P.; Sundstrom, V.; Akesson, E. *Chem. Phys. Lett.* **1999**, *312*, 121.
(15) Jungkamp, T. P. W.; Kirchner, U.; Schmidt, M.; Schindler, R. N. *J. Photochem. Photobiol., A* **1995**, *91*, 1.
(16) Li, Y. M.; Francisco, J. S. *J. Chem. Phys.* **1999**, *111*, 8384.
(17) Schindler, R. N.; Liesner, M.; Schmidt, S.; Kirchner, U.; Benter, T. *J. Photochem. Photobiol., A* **1997**, *107*, 9.
(18) Krisch, M. J.; McCunn, L. R.; Takematsu, K.; Butler, L. J.; Blase, F. R.; Shu, J. *J. Phys. Chem. A* **2004**, *108*, 1650.
(19) Treinin, A.; Hayon, E. *J. Am. Chem. Soc.* **1975**, *97*, 1716.
(20) Chateauneuf, J. E. *Chem. Phys. Lett.* **1989**, *164*, 577.
(21) Jenner, E. L. *J. Org. Chem.* **1962**, *27*, 1031.
(22) Rice, S. A. *Diffusion-Limited Reactions*; Elsevier: Amsterdam, 1985; Vol. 25.
(23) Tachiya, M. *Radiat. Phys. Chem.* **1983**, *21*, 167.
(24) Alfassi, Z. B.; Mosseri, S.; Neta, P. *J. Phys. Chem.* **1989**, *93*, 1380.
(25) Carl, S. A.; Roehl, C. M.; Muller, R.; Moortgat, G. K.; Crowley, J. N. *J. Phys. Chem.* **1996**, *100*, 17191.
(26) The molecular dynamics simulation, based on the work in ref 2, includes one "triatomic" MeOCl molecule that dissociates on an exponential excited state along the OCl coordinate in a bath of 215 fully flexible carbon tetrachloride molecules.
(27) Elles, C. G. Vibrational Relaxation and Photodissociation Dynamics in Solution. Ph.D. Thesis, University of Wisconsin, 2004.
(28) Collins, F. C.; Kimball, G. E. *J. Colloid Sci.* **1949**, *4*, 425.
(29) Solc, K.; Stockmay, W. H. *J. Chem. Phys.* **1971**, *54*, 2981.
(30) Barzykin, A. V.; Shushin, A. I. *Biophys. J.* **2001**, *80*, 2062.
(31) Alfassi, Z. B.; Huie, R. E.; Mittal, J. P.; Neta, P.; Shoute, L. C. T. *J. Phys. Chem.* **1993**, *97*, 9120.
(32) Wendt, H. R.; Hunziker, H. E. *J. Chem. Phys.* **1979**, *71*, 5202.
(33) Fergusson, W. C.; Slotin, L.; Style, D. W. G. *Trans. Faraday Soc.* **1936**, *32*, 956.
(34) Maric, D.; Burrows, J. P.; Meller, R.; Moortgat, G. K. *J. Photochem. Photobiol., A* **1993**, *70*, 205.
(35) Chateauneuf, J. E. *J. Org. Chem.* **1999**, *64*, 1054.
(36) Dneprovskii, A. S.; Kuznetsov, D. V.; Eliseenkov, E. V.; Fletcher, B.; Tanko, J. M. *J. Org. Chem.* **1998**, *63*, 8860.
(37) Raftery, D.; Iannone, M.; Phillips, C. M.; Hochstrasser, R. M. *Chem. Phys. Lett.* **1993**, *201*, 513.
(38) Chateauneuf, J. E. *J. Am. Chem. Soc.* **1990**, *112*, 442.